SF2A 2010
S. Boissier, M. Heydari-Malayeri, R. Samadi and D. Valls-Gabaud (eds)

SPIRE SPECTROSCOPY OF THE INTERSTELLAR MEDIUM

E. Habart[1], E. Dartois[1], A. Abergel[1], J.-P. Baluteau[2], D. Naylor[3], E. Polehampton[3,4], C. Joblin[5] and SAG 4 consortium

Abstract. The SPIRE Fourier Transform Spectrometer on-board Herschel allows us, for the first time, to simultaneously measure the complete far-infrared spectrum from 194 to 671 μm. A wealth of rotational lines of CO (and its isotopologues), fine structure lines of C^0 and N^+, and emission lines from radicals and molecules has been observed towards several galactic regions and nearby galaxies. The strengths of the atomic and molecular lines place fundamental constraints on the physical conditions but also the chemistry of the interstellar medium. FTS mapping capabilities are also extremely powerful in characterizing the spatial morphology of the extended region and understand how the gas properties vary within the studied region. Here, we present a first analysis of SPIRE spectroscopic observations of the prototypical Orion Bar photodissociation region.

Keywords: infrared: ISM, submillimeter: ISM, ISM: lines and bands, ISM: molecules, ISM: clouds, ISM: evolution, ISM: general

1 Introduction

The Orion Bar located between the Orion molecular cloud and the HII region surrounding the Trapezium stars is one of the best-studied photodissociation regions (PDRs) in the Galaxy. Much of the emission from massive star-forming regions will originate from these interfaces, which are responsible for reprocessing the energy output from stars and reemitting this energy at infrared-millimetre wavelengths including a rich mixture of gas lines (i.e., Hollenbach & Tielens 1999). Visible-ultraviolet stellar radiation governs the chemical and thermal state of the gas in these regions. The impinging radiation field on the Bar is χ=(0.5–2.5)$\times 10^4$ χ_0 (Tielens & Hollenbach 1985; Marconi et al. 1998), where χ_0 is the Solar neighbourhood far-UV interstellar radiation field as given by Draine (1978). The UV field varies as a function of depth within the cloud, providing a unique opportunity to study how the dust populations and the molecular content evolve with the excitation and physical conditions. This is important for the evolution of the cloud and its associated star formation.

2 Observations with the FTS

The SPIRE FTS simultaneously measures the source spectrum across two wavebands: Spectrometer Long Wavelength (SLW), covering 14.9 - 33.0 cm^{-1} (303-671 μm) and Spectrometer Short Wavelength (SSW) covering 32.0 - 51.5 cm^{-1} (194-313 μm). Each band is imaged with a hexagonal bolometer array with pixel spacing of approximately twice the beam-width. The Full Width at Half Maximum (FWHM) beam-widths of the SLW and SSW arrays vary between 29 - 42" and 17-21" respectively. The source spectrum, including the continuum, is obtained by taking the inverse transform of the observed interferogram. For more details on the SPIRE FTS instrument, calibration and data reduction procedures, the reader is referred to the articles by Griffin et al. (2010); Swinyard et al. (2010). Our observations are part of the "Evolution of Interstellar dust" key program

[1] Institut d'Astrophysique Spatiale, UMR 8617, CNRS/Université Paris-Sud 11, 91405 Orsay, France
[2] Laboratoire d'Astrophysique de Marseille, UMR6110, CNRS/Université de Provence, 13388 Marseille Cedex 13, France
[3] Institute for Space Imaging Science, University of Lethbridge, Lethbridge, Canada
[4] The Rutherford Appleton Laboratory, Chilton, Didcot OX11 0QX, UK
[5] CESR, UMR5187, CNRS/Université de Toulouse, 31028 Toulouse cedex 4, France

of the SPIRE consortium (Abergel et al. 2010). The Orion Bar was observed with a single pointing in the high-resolution mode of the SPIRE FTS on 2009 September 13 (*Herschel* observation ID, 1342183819). Two scan repetitions were observed which gave an on-source integration time of 266.4 seconds. The unapodized spectral resolution was 0.04 cm^{-1} (1.2 GHz). After apodization (using extended Norton-Beer function 1.5; Naylor & Tahic 2007) the FWHM of the resulting instrument line shape is 0.0724 cm^{-1} (2.17 GHz). While unapodized FTS spectra provide the highest spectral resolution, the instrument line shape, which for an ideal FTS is the classical sinc function, is characterized by relatively large secondary oscillations with negative lobes. An iterative spectral-line fitting routine was developed to extract line parameters from unapodized FTS spectra (Jones et al. 2009).

3 Results

3.1 Detected gas lines

The averaged apodized FTS spectra over the three SLW/SSW detectors aligned on the Bar and corrected for obliquity effects* are presented in Fig. 1. The FTS wavelength coverage allows us to detect a wealth of rotational lines of CO (and its isotopologues), fine structure lines of C and N^+, and emission lines from several radicals and molecules. The expected line positions for detected species are marked in Fig. 1. The ^{12}CO transitions, which appear as the bright narrow lines, are here seen for the first time together from J=4-3 to 13-12 in a single spectrum. The ^{13}CO lines are clearly detected from J=5-4 to 13-12. Most of the $C^{18}O$ lines are visible but blended with the ^{13}CO lines; some $C^{17}O$ lines are detected. One emission line at about 359 μm lies at the position of the fundamental rotational transition of CH^+ (Naylor et al. 2010). This detection can be related to the observation of the CH lambda doublet transitions at about 556.5 μm and 560.7 μm, although it is possibly blended with an HCO^+ $J = 6 \rightarrow 5$ line. The ortho-H_2O $1_{10} \rightarrow 1_{01}$ line at ∼538 and para-H_2 $2_{11} \rightarrow 2_{02}$ at 398 μm are clearly detected. The ∼269 μm para-H_2O $1_{11} \rightarrow 0_{00}$ line was also detected, but the signal-to-noise ratio is low. Some other H_2O lines may be blended. The H_2S $2_{12} \rightarrow 1_{01}$ line at ∼407 μm is detected, while other fainter H_2S lines at shorter wavelengths are only marginally detected. Some features related to the emission of HCO^+, HCN, CN and C_2H are observed as expected (e.g., Hogerheijde et al. 1995; Simon et al. 1997; Young Owl et al. 2000; Teyssier et al. 2004; van Der Wiel et al. 2009), but to help distinguish the spectral confusion for fainter lines or unresolved k-ladder transitions from species such as methanol, the actual signal-to-noise ratio will be improved as the SPIRE FTS response is better understood and, scheduled deeper observations will also help.

3.2 Mapping gas lines

Fig. 1 presents sparse sampled† maps of nearly the complete CO and ^{13}CO band measured. Off-axis calibrations are not guaranteed because both detector arrays have not yet been fully characterised. The comparison between these maps shows the effects of optical depth and excitation in the molecular cloud particularly well. The emission of the less abundant ^{13}CO isotopologue probes the denser shielded regions, while the ^{12}CO optically thick emission likely comes from the less dense surface layers (Lis et al. 1998). The highest rotational lines, which are very sensitive to both gas densities and temperatures, show strong and peaked emission on the Bar, while they are not visible in the off Bar positions. Emission lines of species such as C, N^+ or CH^+ show spatially extended emission.

3.3 Molecular column densities

We used the observed line intensities and the CASSIS software‡ to estimate the beam-averaged molecular column densities. We list in Table 1 column densities estimated for a volume density of 10^5 cm^{-3} as applicable to the extended molecular gas in the Bar (Hogerheijde et al. 1995) and in the high-density limit, because some of

*The obliquity effect is important at the highest frequencies, where a significant error in the line position is introduced.

†The present FTS science demonstration phase observations sparsely samples the field of view and do not allow us to present fully sampled maps.

‡Based on analysis carried out with the CASSIS software and CDMS, JPL spectroscopic databases and RADEX (van Der Tak et al. 2007) molecular databases. CASSIS has been developed by CESR-UPS/CNRS (`http://cassis.cesr.fr`).

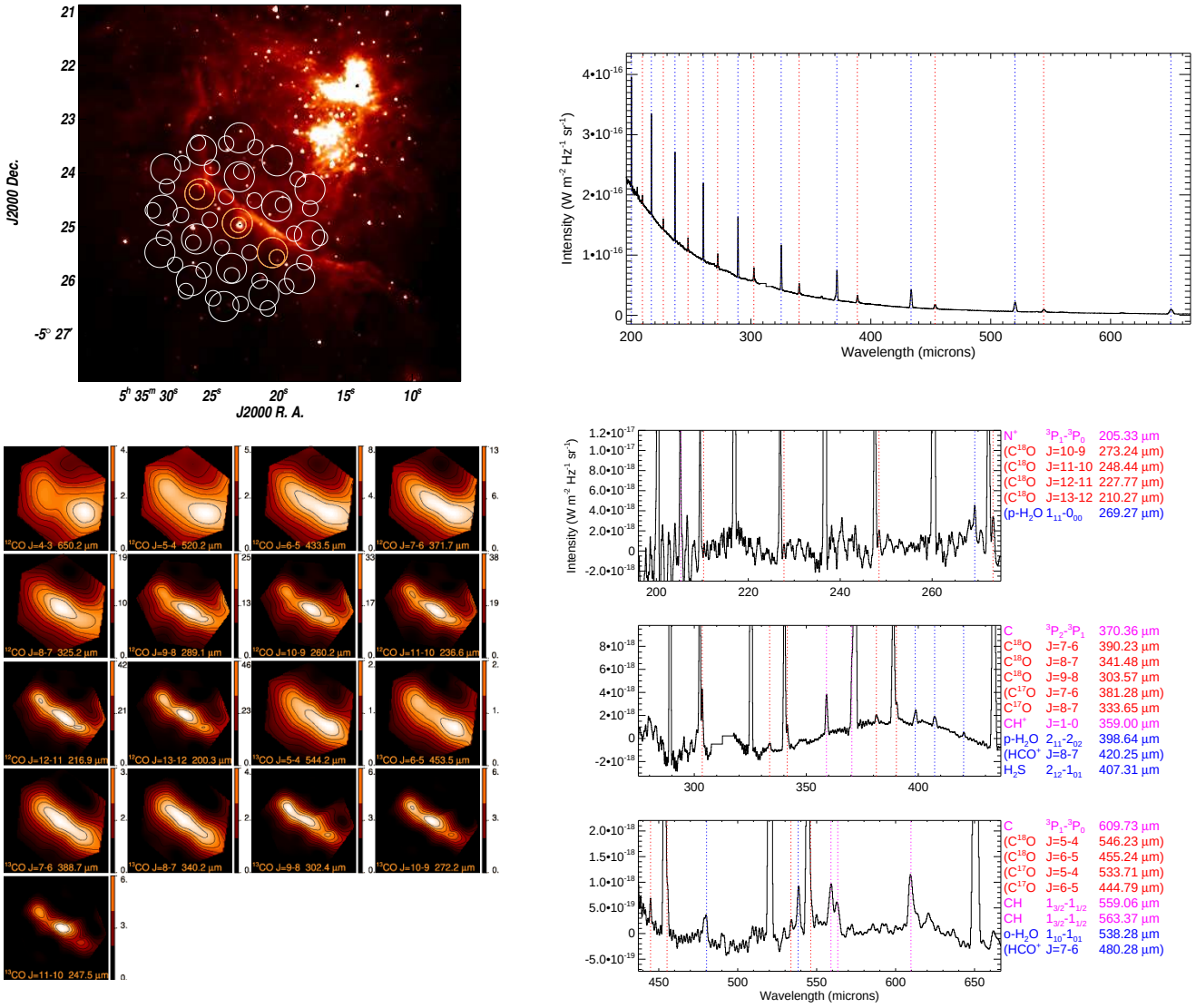

Fig. 1. Upper left : Map of the Orion Bar obtained with Spitzer (IRAC at 3.8 μm) with the SPIRE SLW (large circle) and SSW (small circle) array positions marked. The three arrays on the Bar are marked by yellow large and small circles. The PDR is wrapped around the HII region created by the Trapezium stars (right corner) and changes from a face-on to an edge-on geometry where the emission peaks. Upper right : Averaged apodized FTS spectra over the three arrays on the Bar. The blue and red dotted lines delinate the ^{12}CO and ^{13}CO lines position respectively. Lower right : Zoom of the averaged apodized FTS spectra continuum substracted. Dotted lines show the positions where specific gas lines are expected, excluding the ^{12}CO and ^{13}CO lines. The corresponding lines and wavelengths are marked on the right. Lines between brackets are only possibly detected at this level of analysis. Lower left : Sparse sampled maps in the ^{12}CO and ^{13}CO lines measured, except for the ^{13}CO $J = 12 - 11$ at ∼227 and $J = 13 - 12$ at 209 μm lines. Scales are in 10^5 erg s^{-1} cm^{-2} sr^{-1}. Contour levels are drawn at 10, 20,..., 90 % of the maximum intensity.

the line emission may originate from dense clumps[§]. We adopt the mean molecular gas temperature towards the Bar of ∼85 K for kinetic temperatures as determined from the ground Hogerheijde et al. (1995), and the more extreme 50 to 150 K range values that probe different zones of the PDR (Lis & Schilke 2003; Batrla & Wilson 2003). The line widths were taken equal to 3 km s^{-1}, following previous higher resolution observations

[§]The clumpiness of the PDR inferred by Hogerheijde et al. (1995) was confirmed by interferometric data of Young Owl et al. (2000); Lis & Schilke (2003). Clump densities up to 10^7 cm^{-3} were derived by Lis & Schilke (2003), while the density of the interclump medium should fall between a few 10^4 cm^{-3} (Young Owl et al. 2000) and 2 10^5 cm^{-3} (Simon et al. 1997).

(Hogerheijde et al. 1995; Johnstone et al. 2003). Our values for the column densities agree for species detected from the ground with previously published values to within a factor of $2-3$: Hogerheijde et al. (1995) for $C^{18}O$ and HCO^+; Johnstone et al. (2003) for $C^{17}O$; and Leurini et al. (2006) for H_2S. Beam dilution effects could introduce a significant factor. To convert the observed $C^{18}O$ J=8-7 and $C^{17}O$ J=8-7 line intensities to a total H_2 column density, we assume isotopic ratios $^{16}O/^{18}O\sim560$, $^{16}O/^{17}O\sim1800$ (Wilson & Rood 1994) and a relative CO abundance to H_2 of 1.1×10^{-4} as applicable for the Orion Bar PDR (Johnstone et al. 2003). We find $N(H_2)\sim9\ 10^{22}$ cm^{-2} assuming $T\sim85$ K, which implies the following molecular abundances on the Bar: x(ortho-H_2O)$\leq3.3^{+3.3}_{-1.7}\ 10^{-7}$; x(para-$H_2O$)$\leq5^{+11.7}_{-3.1}\ 10^{-7}$; x($HCO^+$)$\leq3.9^{+8.3}_{-2.1}\ 10^{-9}$; x($CH^+$)$=7.2^{+2.6}_{-0.7}\ 10^{-11}$; x($H_2S$)$=3.4^{+2.3}_{-1}\ 10^{-10}$. H_2O is extremely sensitive to the local physical conditions in molecular clouds: close to the surface, molecules are photodissociated, while deeper into the cloud molecules freeze onto grain surfaces (i.e., Hollenbach et al. 2009). Desorption of ices (Westley et al. 1995; Seperuelo Duarte et al. 2009) could supply gas-phase species. The high abundances of sulphur species remain an interesting puzzle for interstellar chemistry (i.e., Goicoechea et al. 2006). The observed abundance of species such as H_2S are difficult to interpret in models. H_2S results from a mixed chemistry involving gas-phase reactions and grain-related processes.

Table 1. Beam-averaged molecular column densities.

Species	Transition	Wavelength (microns)	E_u (K)	Intensity[a] (10^{-6} erg s^{-1} cm^{-2} sr^{-1})	Column density (10^{15} cm^{-2})
$C^{18}O$	$J=7\rightarrow6$	390.2	147.5	2.6[1.1]	7.7[24,3.8][b]
$C^{18}O$	$J=8\rightarrow7$	341.5	189.6	3.3[1.1]	15[72,5.5][b]
$C^{18}O$	$J=9\rightarrow8$	303.6	237.0	11[3.9]	96[720,25][b] - 10[43,5.4][c]
$C^{17}O$	$J=8\rightarrow7$	333.7	194.1	1.4[1.1]	6.6[33,2.3][b]
CH^+	$J=1\rightarrow0$	359.0	40.1	6.7[1.1]	0.0065[0.0058,0.0088][c]
ortho-H_2O	$1_{10}\rightarrow1_{01}$	538.3	61.0	2.6[1.1]	$\leq$30[60,15][b,d]
para-H_2O	$2_{11}\rightarrow2_{02}$	398.6	136.9	2.0[1.1]	$\leq$45[150,17][b,d]
HCO^+	$J=8\rightarrow7$	420.3	154.1	≤0.7[e]	$\leq$0.35[1.1,0.16][b,e]
H_2S	$2_{12}\rightarrow1_{01}$	407.3	55.1	1.4[1.1]	0.031[0.023,0.052][c]

(a): Intensities with uncertainty in between brackets. (b): Beam-averaged column densities using RADEX with $n=10^5$ cm^{-3} and T=85 K, with estimations for 50 and 150 K in between brackets. (c): Beam-averaged column densities in the high-density (LTE) limit for 85 K, with estimations for 50 and 150 K in between brackets. (d): Note that the density (or temperature) could be higher than assumed, which would decrease the column density, and the para-H_2O $2_{11}\rightarrow2_{02}$ line could be affected by IR pumping. (e): We used the HCO^+ $J=8\rightarrow7$ line because the HCO^+ $J=7\rightarrow6$ line is possibly blended with an HCl $J=1\rightarrow0$ line. Column densities from ^{12}CO and ^{13}CO lines are uncertain due to high optical depth and are not listed.

4 Conclusions

We have analysed the first spectral survey taken in the Orion Bar by the FTS of SPIRE. A wealth of rotational lines of CO (and its isotopologues), fine structure lines of C and N^+, and emission lines from radicals and molecules such as CH^+, CH, H_2O or H_2S were found. For species detected from the ground, our estimates of the column densities agree with previously published values. The comparison between ^{12}CO and ^{13}CO maps shows particularly the effects of optical depth and excitation in the molecular cloud. The distribution of the ^{12}CO and ^{13}CO lines with upper energy levels is discussed in Habart et al. (2010). Fully sampled map will be investigated in the near future. SPIRE/FTS data should be associated to PACS and HIFI data. In particular, observations of gas cooling lines at high spectral resolution with HIFI will allow us to assign some lines that could be merged in the lower resolution SPIRE spectra and provide missing information about the gas velocity within the PDR.

References

Abergel, A, Arab, H, Compiègne, M, et al. 2010, *A&A*, 518:L96.
Batrla, W & Wilson, T. L. 2003, *A&A*, 408:231.

Draine, B. T. 1978, *Astrophysical Journal Supplement Series*, 36:595.

Goicoechea, J. R, Pety, J, Gerin, M, Teyssier, D, Roueff, E, Hily-Blant, P, & Baek, S. 2006, *A&A*, 456:565.

Griffin, M. J, Abergel, A, Abreu, A, et al. 2010, *A&A*, 518:L3.

Habart, E, Dartois, E, Abergel, A, et al. 2010, *A&A*, 518:L116.

Hogerheijde, M. R, Jansen, D. J, & Van Dishoeck, E. F. 1995, *A&A*, 294:792.

Hollenbach, D. J & Tielens, A. G. G. M. 1999, *Reviews of Modern Physics*, 71:173.

Hollenbach, D, Kaufman, M. J, Bergin, E. A, & Melnick, G. J. 2009, *ApJ*, 690:1497.

Johnstone, D, Boonman, A. M. S, & van Dishoeck, E. F. 2003, *A&A*, 412:157.

Jones, S, Naylor, D, Gom, B, & Spencer, L. 2009, *Proc. 30th Canadian Symposium on Remote Sensing.*

Leurini, S, Rolffs, R, Thorwirth, S, Parise, B, Schilke, P, Comito, C, Wyrowski, F, Güsten, R, Bergman, P, Menten, K. M, & Nyman, L. A. 2006, *A&A*, 454:L47.

Lis, D. C & Schilke, P. 2003, *ApJ*, 597:L145.

Lis, D. C, Serabyn, E, Keene, J, Dowell, C. D, Benford, D. J, Phill, T. G, Hunter, T. R, & Wang, N. 1998, *ApJ*, 509:299.

Marconi, A, Testi, L, Natta, A, & Walmsley, C. M. 1998, *A&A*, 330:696.

Naylor, D & Tahic, M. 2007, *J. Opt. Soc. Am. A 24, 3644-3648.*

Naylor, D, Dartois, E, Habart, E, et al. 2010, *A&A*, 518:L117.

Seperuelo Duarte, E, Boduch, P, Rothard, H, Been, T, Dartois, E, Farenzena, L. S, & Da Silveira, E. F. 2009, *A&A*, 502:599.

Simon, R, Stutzki, J, Sternberg, A, & Winnewisser, G. 1997, *A&A*, 327:L9.

Swinyard, B, Ade, P, Baluteau, J, et al. 2010, *this issue.*

Teyssier, D, Fossé, D, Gerin, M, Pety, J, Abergel, A, & Roueff, E. 2004, *A&A*, 417:135.

Tielens, A. G. G. M & Hollenbach, D. 1985, *ApJ*, 291:722.

van Der Tak, F. F. S, Black, J. H, Schoeier, F. L, Jansen, D. J, & van Dishoeck, E. F. 2007, *A&A*, 468:627.

van Der Wiel, M. H. D, van Der Tak, F. F. S, Ossenkopf, V, Spaans, M, Roberts, H, Fuller, G. A, & Plume, R. 2009, *A&A*, 498:161.

Westley, M. S, Baragiola, R. A, Johnson, R. E, & Baratta, G. A. 1995, *Nature*, 373:405.

White, G. J & Sandell, G. 1995, *A&A*, 299:179.

Wilson, T. L & Rood, R. 1994, *ARA&A*, 32:191.

Young Owl, R. C, Meixner, M. M, Wolfire, M, Tielens, A. G. G. M, & Tauber, J. 2000, *ApJ*, 540:886.